

Parametric Design and Field Behavior of Earthen Structures

R. Paranthaman¹ and S. Azam^{1*}

¹ *Environmental Systems Engineering, Faculty of Engineering and Applied Science, University of Regina,
3737 Wascana Parkway, Regina, SK S4S 0A2, Canada*

Received 14 February 2023; revised 18 March 2023; accepted 22 March 2023; published online 30 April 2023

ABSTRACT. The stability of earthen structures is governed by field uncertainties arising from material properties, environment loading, and slope geometry. This research devised a systematic approach to capture the effects of field uncertainties on the stability of natural and manmade slopes. New design charts were developed by incrementally changing slope geometry and randomly generating shear strength parameters. Subset simulation was used to determine the safe range of soil properties for various slopes. The charts were applied to three published case studies with distinct triggering mechanisms resulting from complex field settings. All of the investigated slopes were found to be stable (factor of safety (FOS) > 1.0) under the reported geometry and shear strength parameters while assuming no water table. The effects of soil properties' variation and environmental conditions on fluctuating water table were captured through history matching. Results indicated three distinct failure mechanisms: foundation settlement of a glacial moraine till (Vernon, British Columbia) due to an increased pore water pressure during construction of the compacted fill (FOS = 1.45 without berms and 2.24 with berms); instability in the natural cut (FOS = 0.98) comprising layered glacio-lacustrine clays (Labret, Saskatchewan) due to saturation of the entire slope resulting from a long duration rainfall; and collapse of a compacted fill (FOS = 0.98) on a glacial moraine till (Hamelin Creek, Alberta) due to soil saturation arising from thawing of a frozen layer in the slope. This validation illustrates that the new approach fully captures environmental loading (resulting in water table variation in the slope) and partly captures construction practice and site geology via soil properties.

Keywords: slope stability, parametric design, soil properties, environmental loading

1. Introduction

Civil infrastructure supported by earth materials inherently involve uncertainties throughout their lifecycle (design, construction, and performance). The design is based on the factor of safety (FOS) against failure which ensures that the resisting force (material strength) exceeds the driving force (material weight) (Morgenstern and Price, 1965). The shear strength of a soil is derived from friction between particles and cohesion of clay minerals (Mitchell and Soga, 2005). Likewise, the soil weight increases when water is added to it due to precipitation. The FOS uses conservative assumptions to account for uncertainties in soil properties and soil saturation at a given location (Davies, 2015). Generally, the resulting structures have large footprints along with huge material volumes requiring longer time and more funds for construction (Bogusz and Godlewski, 2019). Therefore, there is a need for a parametric analysis to ensure stable earth structures while efficiently using materials and their properties.

The uncertainties are related to soil properties and weights (cohesion, c ; friction angle, ϕ ; unit weight, γ_b) thereby re-

sulting in distress and failure of earthen embankments (Chowdhury, 2013). The various factors affecting the uncertainties at a site include one or more of the following: (i) limited and unreliable field data for spatially distributed earth structures; (ii) difficulties in the quantification of three dimensional variability in soil parameters (Malkawi et al., 2000); (iii) inadequate capability of numerical models and empirical equations to simulate natural phenomena (Glade, 2003); (iv) insufficient quality control and quality assurance during construction. To increase FOS, detailed design takes into consideration the geology and geohydrology of the terrain as well as the geometry of the structure. Moreover, the slopes are exposed to environmental loading (such as prolonged rainfall, water table (WT) rise, snow melt in spring, and soil freezing during winter) thereby aggravating their field performance. The various types of uncertainties have resulted in embankment failure such as track derailment near Togo (Saskatchewan, Canada) (Transportation Safety Board, 2013) and lateral slope movement of 40 mm near Lac La Biche (Alberta, Canada) (Wang et al., 2012). Clearly, a detailed assessment through a systematic approach is required to reduce the impairment of civil infrastructure in light of uncertainties.

The classical approach for slope stability analysis is to determine FOS using limit equilibrium methods (LEM). Based on shear strength parameters (cohesion and friction), this approach does not capture variability in soil properties. To account for

* Corresponding author. Tel.: 01-306-337-2369; fax: 1-306-585-4855.
E-mail address: shahid.azam@uregina.ca (S. Azam).

Table 1. Summary of Statistical Approaches for Probabilistic Assessment of Slope

Approach/References	Description	Limitations
Approximation Methods		
Point estimation method (PSM) (Harr, 1984; Li, 1992; Wang and Huang, 2012)	Uses a series of point-by-point estimation of the performance function at selected input variable; Requires mean and variance of all inputs; Performance functions to define FOS	Ignore spatial variability by indirectly assuming perfect correlation, use of predefined critical surface, and under estimation of P_f
First-order second-moment (FOSM) (Tang et al., 1976; Christian et al., 1994; Hassan and Wolff, 1999)	Based on Taylor series expansion of the performance function to define FOS; Uses Mean and variance of all inputs	Same as above
Analytical Methods		
First-order reliability method (FORM) (Low et al., 1998; Low and Tang, 2007; Cao and Wang, 2014)	Based on multivariate distribution of the input variables and mathematical function to define FOS	Limitation in the optimization tool in spread sheet and under estimation of P_f
Jointly distributed random variable (JDRV) (Johari and Javadi, 2012; Johari and Khodaparast, 2013; Johari and Mousavi, 2019)	Based on probability distribution function (PDF) of input variables and mathematical function to define FOS	Sophisticated correlations and require powerful computation
Simulation Methods		
Response surface method (RSM) (Li et al., 2011; Huang and Zhou, 2017; Zhou and Huang, 2018)	Produces failure surface using the input variables using mathematical function and models by finite element to define FOS	Point estimation to generate response and approximation functions in surface generation
Monte Carlo simulation (MCS) (El-Ramly et al., 2002; Griffiths et al., 2009; Zhang et al., 2011)	Repeated random samples generation using PDF of input variables. mathematical function to define FOS	Need for large amount of random samples and longer time for computations
Subset simulation (SS) (Au and Beck, 2003; Wang et al., 2011; Li et al., 2016)	Makes use of conditional probability and Markov chain levels to compute FOS using PDF of input variables	Need spreadsheet to estimate the new confining range for each input at each level

such unpredictability, LEM is combined with statistical analysis thereby determining the failure probability (P_f) of slopes (Wang et al., 2011; Cao, 2012). These approaches are summarized in Table 1. The approximation methods assume perfect correlation between spatial variability, use a predefined critical surface, and generally underestimate P_f (Cao, 2012). The analytical methods use random samples using a probability distribution function (PDF) of soil properties along with LEM to evaluate P_f . The shortcomings include constraints in result optimization and P_f underestimation in first-order reliability method (FORM) and complex correlations and computational power requirement in jointly distributed random variable (JDRV). The simulation methods generate numerous random samples within the maximum and minimum ranges of soil properties to estimate P_f . The response surface method (RSM) produces a failure surface using the input variables and the accuracy is limited by point estimation between responses and approximation functions (Jahnavi, 2016; Johari and Mousavi, 2019). The Monte Carlo simulation (MCS) provides a range of possible outcomes and the corresponding probabilities of occurrence to address the risk in relation to uncertainties in quantitative analysis. This method is limited by the need of advanced computational facility and longer time for computations to improve the efficiency and resolution (Jiang et al., 2014). As part of MCS, the newly developed subset simulation examines the rare failure scenarios into a sequence of more frequent ones (Au and Beck, 2003; Wang et al., 2011). This generates larger conditional probabilities for accurate computation of P_f with smaller number of scenarios.

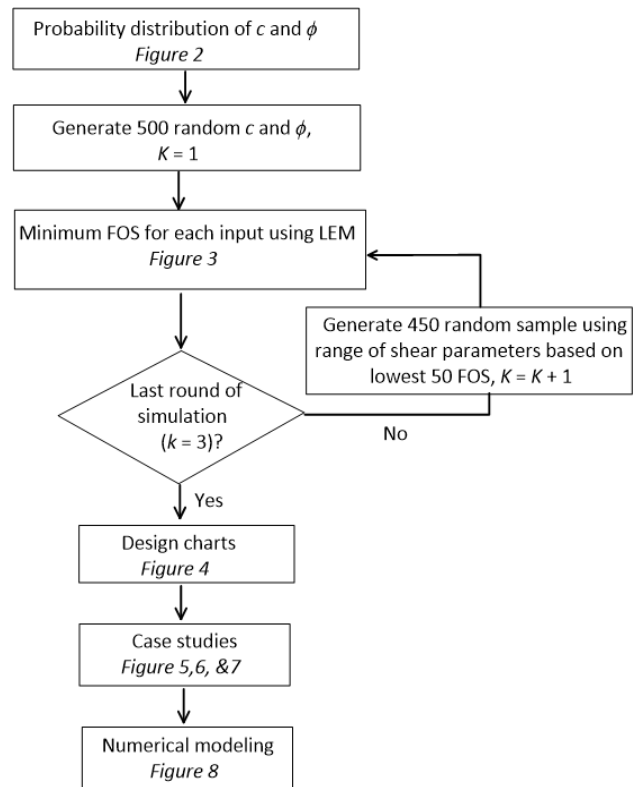


Figure 1. Flow chart for parametric design and field behavior of earthen structures.

The main objective of this paper was to develop a parametric design approach for understanding field behavior of earthen structures. Design charts were developed by incrementally changing slope geometry and randomly generating shear strength parameters. For this purpose, the subset simulation technique was used to determine the safe range of soil properties for various slopes. The charts were applied to three published failures with distinct triggering mechanisms resulting from complex field settings (construction, geology, and environment). To validate the new approach, history matching was conducted through parametric analyses of soil properties and/or water table using a numerical model for slope stability.

2. Research Methodology

Design charts were developed as graphical tools to determine FOS based on step-wise approach of using slope geometries along with soil properties. Figure 1 gives the flow chart for parametric analysis on slope stability. A typical slope of earthen embankment with varying heights (H , 5 ~ 30 m at 5 m increments) and slope angles (α , 30° ~ 60° at 10° increments) was selected for the development of design charts. The reported values of parameters for material strength (c and ϕ) for soils across the northern hemisphere were collected and the data were converted to normal distribution functions (Figure 2) according to the following equation:

$$f(x) = \frac{1}{\sqrt{2\pi}s^2} e^{-\frac{(s-\mu)^2}{2s^2}} \quad (1)$$

In the above equation, s is the standard deviation, S is the shear strength parameter (c or ϕ), and μ is the arithmetic mean. The reported c (0 ~ 40 kPa) and ϕ (11° ~ 40°) values cover the range of soil types across the globe (Holtz et al., 2011; Das and Sobhan, 2013). Cohesion is derived from the interactions of negatively charged minerals with bipolar water molecules and is responsible for the sticky nature of the clayey portion of a soil (Mitchell and Soga, 2005). Likewise, friction angle is generated due to the interlocking of silt and sand particles in a soil (Hillel, 1998).

For a given slope geometry, subset simulation (Figure 3) was performed using three iterations (k) to identify the possible failure range based on shear strength parameters. Initially ($k = 1$), 500 discrete random cohesion and friction angle values were generated from the probability distribution functions (PDFs) to identify potential failure scenarios. Under each scenario, the FOS was predicted following the LEM using dimensionless charts (Hoek and Bray, 1981; Wyllie, 2018). The slope stability analyses (numerical solution of LEM equations) were conducted using an Excel workbook developed by Carranza-Torres and Hormazabal (2018). This workbook uses material strength parameters along with the Bishop method, which considers normal forces and moment equilibrium to determine FOS (Cheng and Lau, 2008). Denoting σ for applied stress and u_w for pore water pressure, the shear strength (τ) of a soil is based on the Mohr-Coulomb failure criterion and is described according to the fol-

lowing equation (Holtz et al., 2011):

$$\tau = c + (\sigma - u_w) \tan \phi \quad (2)$$

The effective stress ($\sigma - u_w$) for a soil decreases with an increase in u_w due to ground water rise or infiltration from surface water and precipitation. The increase in pore water pressure reduces the load carrying capacity of a soil thereby decreasing the shear strength (Terzaghi et al., 1996).

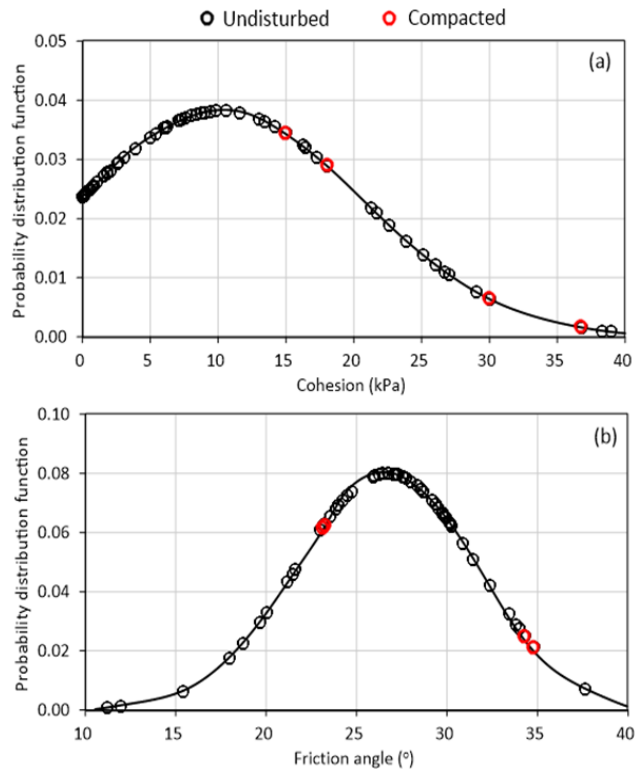


Figure 2. Probability distribution functions of reported soils in the northern hemisphere: (a) cohesion and (b) friction angle [data obtained from Vanapalli et al. (1997), Bell (2002), MDH (2010), Oh and Vanapalli (2010), and Clarke (2018)].

Table 2. Stability Analysis of Selected Case Studies Using Design Chart

Case Study	Location and Reference	Slope Height (m)	Slope Angle (°)	Cohesion (kPa)	Friction Angle (°)	FOS
I	Vernon, British Columbia (Crawford et al., 1995)	11.0	33.7	10.0	33.0	≥ 1
II	Labret, Saskatchewan (Donnelly et al., 2019)	20.0	24.0	20.0	28.0	≥ 1
III	Hamelin Creek, Alberta (Tweedie et al., 2004)	24.0	33.3	18.0	18.0	≥ 1

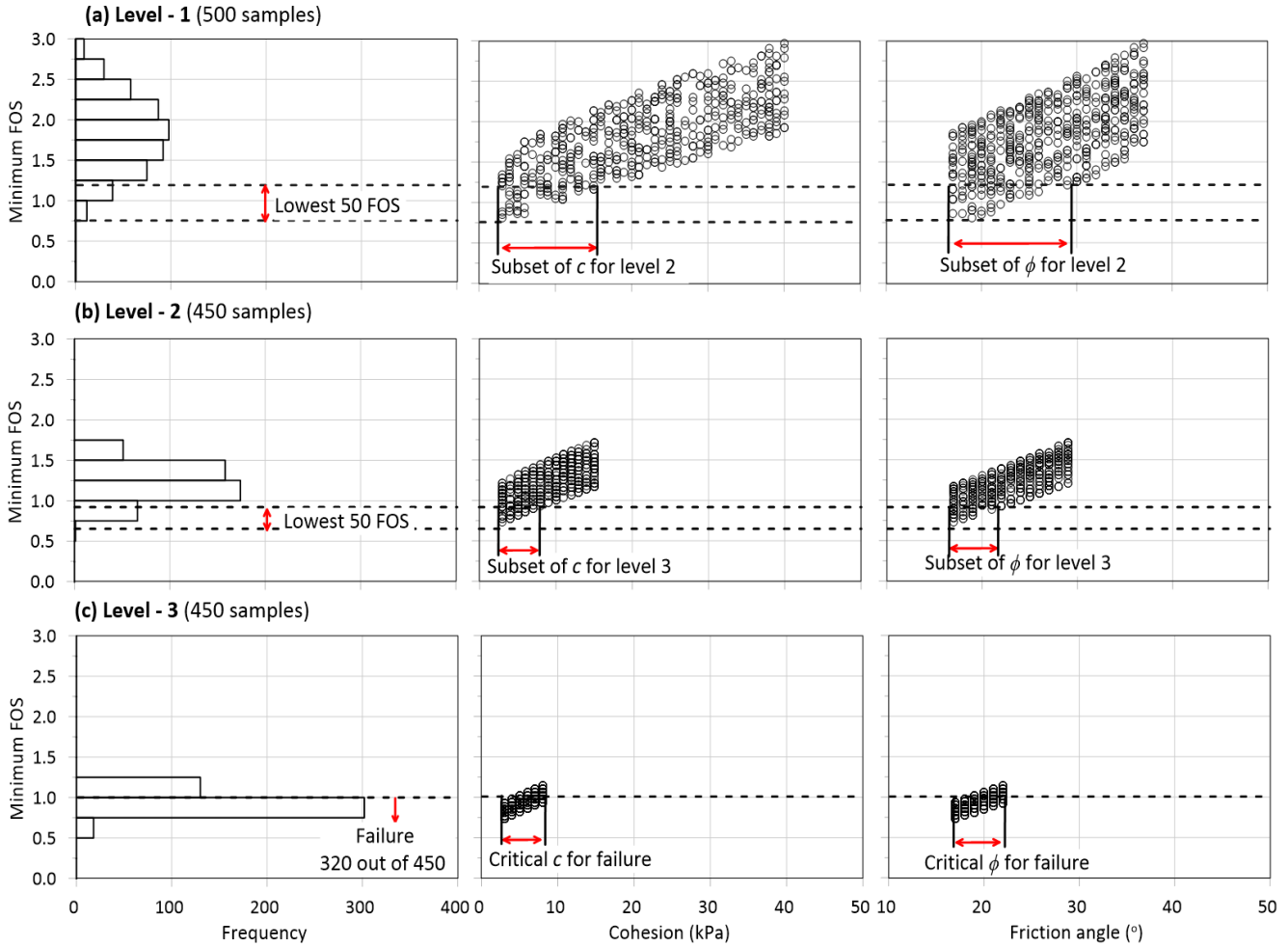


Figure 3. Minimum FOS versus frequency, cohesion, and friction angle during the simulation process ($H = 15\text{ m}$ and $\alpha = 30^\circ$) for three iterations: (a) $k = 1$; (b) $k = 2$; (c) $k = 3$.

Table 3. Detailed Summary of Environmental Factors for Case Study

Case Study	Construction Type	Site Geology (CSSS, 2023)	Environmental Conditions			Failure Mechanism	
			Climate Classification and Seasonal Weather*	Pre-failure Precipitation	Surface Water		Water Table
I	Compacted Fill	Glacial Moraine Till	Dfb S-S ($P = 35\text{ mm}$; $T = 16.1\text{ }^\circ\text{C}$) F-W ($P = 34\text{ mm}$; $T = 2.4\text{ }^\circ\text{C}$)	10 mm in June 1989 and none in March 1990	Swan Lake located 400 m away for surface runoff	0 ~ 2 m below ground	Excess pore pressure builds up in foundation soil during construction
II	Natural Cut	Glacio-lacustrine Clay	Dfc S-S ($P = 52\text{ mm}$; $T = 17.1\text{ }^\circ\text{C}$) F-W ($P = 13\text{ mm}$; $T = -10.2\text{ }^\circ\text{C}$)	124 mm rainfall in 23 days	Qu'Appelle Valley Lake (100 m away and 18 m below) for surface runoff	0 ~ 6 m below slope	Saturation of slope from the surface downward long after the construction
III	Compacted Fill	Glacial Moraine Till	Dfb S-S ($P = 52\text{ mm}$; $T = 19.6\text{ }^\circ\text{C}$) F-W ($P = 10\text{ mm}$; $T = -10.0\text{ }^\circ\text{C}$)	16 mm snowfall in 10 days	Hamelin Creek underlying for surface runoff	None	Thawing of frozen layer causing saturation at interface within the slope during construction

Note: *S-S = Spring-Summer (April to October), F-W = Fall-Winter (November to March), P = Precipitation, T = Air temperature, Dfb = warm summer humid continental climate, Dfc = cold arctic climate.

Next ($k = 2$), all previously obtained FOS were sorted in decreasing order and the range for cohesion and friction angle corresponding to 50 lowest FOS scenarios (10% of 500 scenarios) were used to generate 450 new failure scenarios. This refinement increased the accuracy in determining P_f (Li et al., 2016). Finally ($k = 3$), the above processes were repeated to optimize enhanced accuracy and computational time (Wang et al., 2011). The resulting FOS was used to generate design charts (Figure 4) for selected slope geometries.

The newly developed design charts were applied to three failed slopes (Vernon British Columbia, Labret Saskatchewan,

and Hamelin Creek Alberta) reported in the literature. As mentioned earlier, these case studies were selected to understand the distinct trigger mechanisms of slope failures resulting from complex field settings such as construction practice, site geology, and environmental loading. Table 2 gives the simplified stability analysis using the design charts. Based on the average shear strength parameters and given geometry, these dry slopes were found to be stable (FOS > 1.0). Utilizing the existing slope geometry, history matching was conducted to understand the effect of soil properties and environmental loading (Table 3) on the stability of the selected case studies. For this purpose, para-

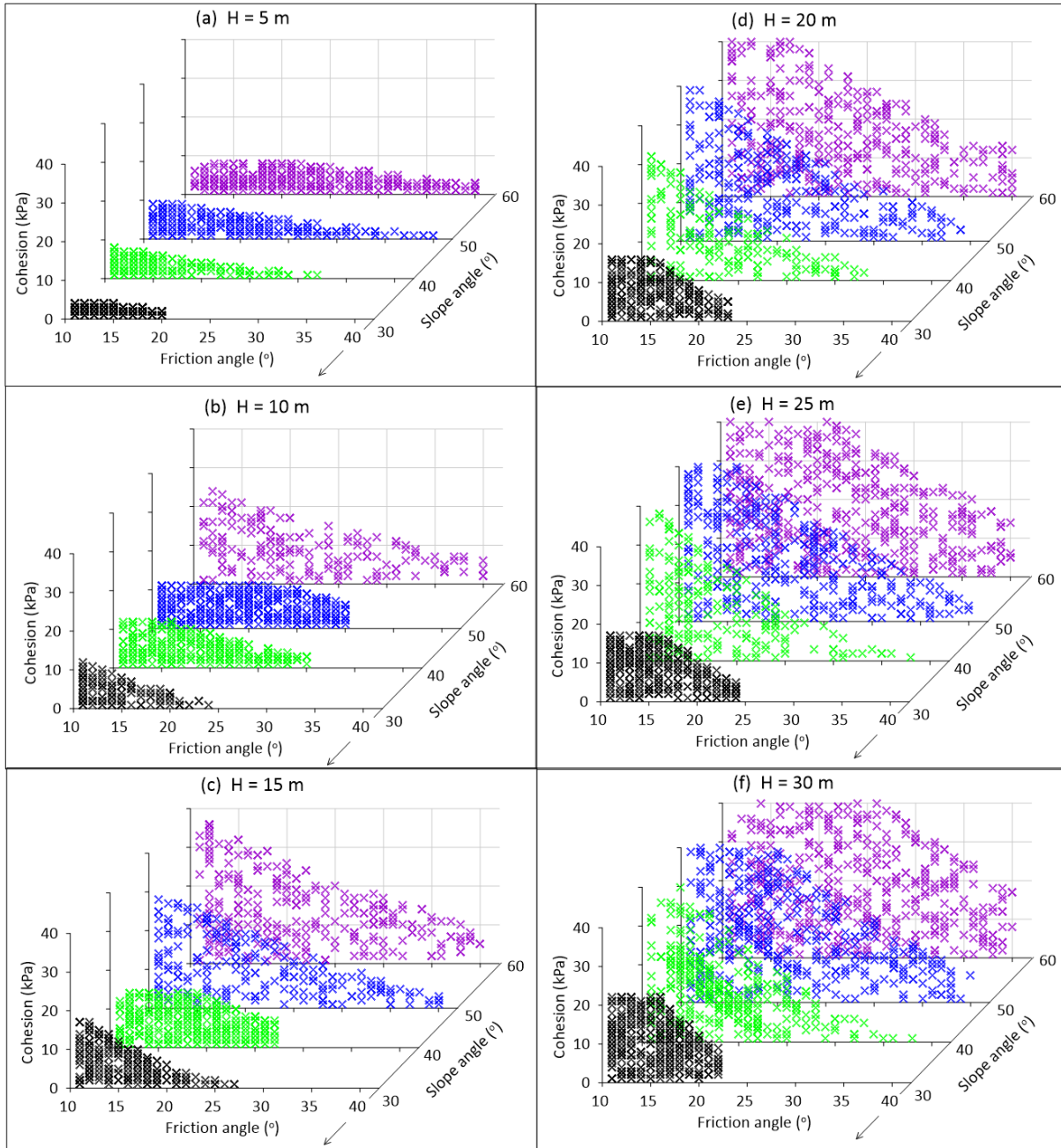


Figure 4. Design charts for dry slope with various slope height: (a) 5 m; (b) 10 m; (c) 15 m; (d) 20 m; (e) 25 m; (f) 30 m.

metric analyses were conducted using a numerical slope stability software (Geostudio Slope/W). This model used shear strength parameters as before along with the Morgenstern-Price method (Morgenstern and Price, 1965), which accounts for shear and normal forces as well as moment and force equilibrium to determine FOS. To understand the causes of failure, each case study was analysed in further detail.

3. Case Studies

3.1. Case Study I – Vernon, British Columbia

Figure 5 gives the slope stability investigation for the case study at Vernon, British Columbia. This new road was constructed over a silty clay soil (glacial moraine deposits) intersecting Highway 97 at the north end of the town. The soil properties were $10 \leq c \leq 30$ kPa, $33^\circ \leq \phi \leq 35^\circ$, and an average $\gamma_b = 20.3$ kN/m³ (Crawford et al., 1995). Although this region receives a monthly average precipitation of 35 mm, the one-month rainfall preceding the first failure (June 1989) was only 10 mm and that preceding the second failure (March 1990) was zero (Canada Weather Stats, 2023). This means that the shallow ground water table (0 ~ 2 m below the embankment) was due to a close proximity to the Swan Lake (400 m from the slope) and not due to infiltration.

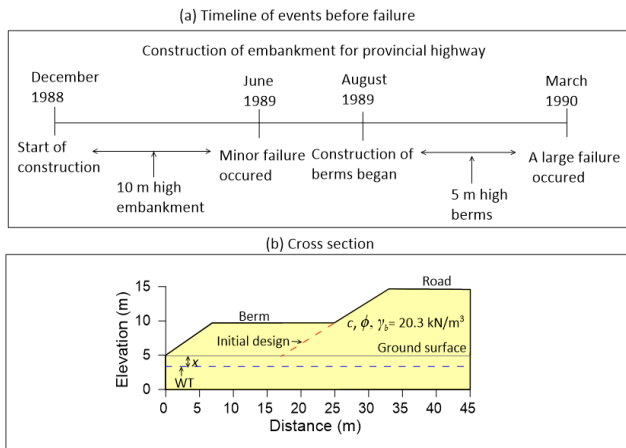


Figure 5. Summary of slope stability at Vernon, British Columbia (Crawford et al., 1995): (a) timeline of events before slope failure and (b) typical cross section of the slope.

Based on Crawford et al. (1995), construction began in December 1988 along with monitoring for pore pressure and settlement as the height was gradually increased. The initial fill placement was at a rate of 1.5 m/month for three months and this rate was increased to 3.0 m/month thereafter such that a 10 m height was constructed by June 1989. At that time, a failure on the north-side of the embankment displaced 3500 m³ of material along with a settlement of up to 4 m. This slope failure was attributed to variation in soil properties and pore pressure increase in the sub-surface silty clay, which required longer time than that allowed by the construction schedule. To mitigate, 5.0 m high berms were constructed on both sides of the road during

August 1989 and March 1990. When the final 0.4 m was placed, a larger failure occurred on both sides of embankment: details of displaced materials and settlement were not reported. This failure was attributed to excess pore pressure build up in the foundation soil during construction. This time, the road was completed by using a light-weight backfill to decrease applied stresses along with wick drains to dissipate excess pore water pressure from the subsurface.

3.2. Case Study II – Labret, Saskatchewan

Figure 6 gives the detailed slope stability investigation for the case study at Labret, Saskatchewan. This existing highway was constructed using natural cut method in a glacio-lacustrine deposits with layered clayey soil ($0 \leq c \leq 25$ kPa, $25^\circ \leq \phi \leq 35^\circ$, and $13.7 \leq \gamma_b \leq 20.1$ kN/m³) as part of the provincial highway No. 56-02-40 (Donnelly et al., 2019). The pre-failure rainfall was more than double (124 mm) in July 2012 when compared with the monthly average rainfall of 52 mm during spring-summer. Furthermore, the Qu'Appelle Valley Lake is located 100 m away at a depth of 18 m from the embankment surface thereby precluding the influence of ground water table on the failure of the slope.

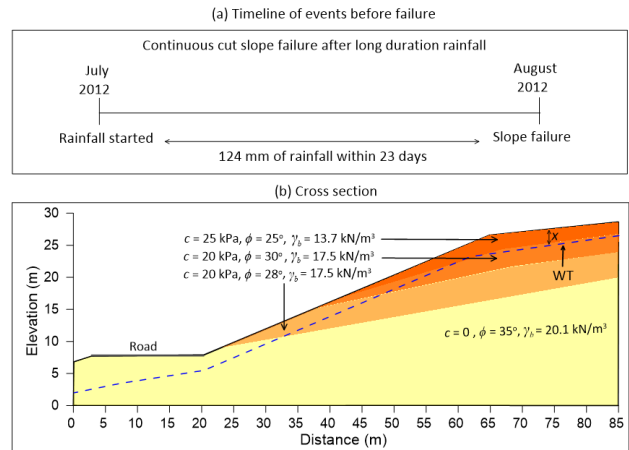


Figure 6. Summary of slope stability at Labret, Saskatchewan (Donnelly et al., 2019): (a) timeline of events before slope failure and (b) typical cross section of the slope.

Based on Donnelly et al. (2019), a slope failure was reported in 2012 on the south-side of the embankment across the highway. The failure occurred following 23 days (from July 11, 2012 to August 2, 2012) of rain at a nominal intensity of 5 mm/day and including 5 days of up to 12 mm/day intensity. Therefore, saturation of slope from surface downward was the likely triggering mechanism. A rehabilitation project was carried out in 2013 ~ 2015 comprising of the following: driving 12 m piles into the natural soil slope; excavation of loose soil to a depth of 0.5 m and backfilling with granular soil; and installation of guardrails.

3.3. Case Study III – Hamelin Creek, Alberta

Figure 7 gives the detailed stability investigation for the case study at Hamelin Creek, Alberta. This 24 m high embankment

was constructed on a glacial moraine deposit along Highway 725 crossing the Creek Valley using clayey soil ($6 \leq c \leq 18$ kPa, $18^\circ \leq \phi \leq 20^\circ$, and an average $\gamma_b = 18$ kN/m³). Although this region receives a monthly average precipitation of 52 mm along with an air temperature of 19.6 °C during spring-summer, an unprecedented 16 mm of snowfall was recorded over the month of May 2003 prior to the failure. The intersecting Hamelin Creek Valley occasionally receives surface runoff in spring (melt-water) and summer (rainwater) thereby precluding a distinct ground water table.

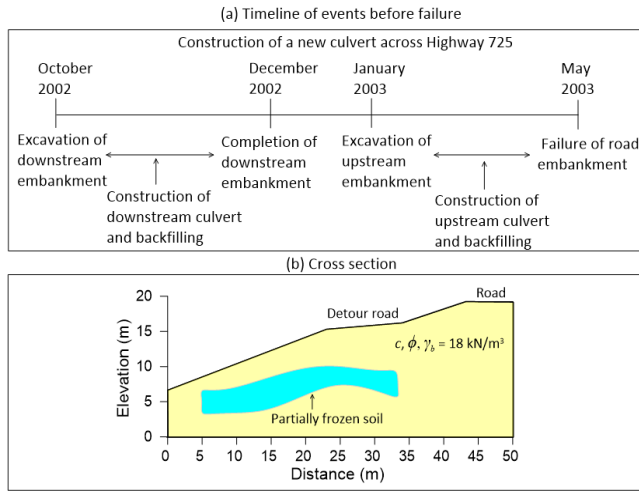


Figure 7. Summary of slope stability at Hamelin Creek, Alberta (Tweedie et al., 2004): (a) timeline of events before slope failure and (b) typical cross section of the slope.

According to Tweedie et al. (2004), the replacement of two culverts under this embankment began in October 2002. Construction activities (excavation, laying of culverts, and backfilling) started on the downstream side and gradually completed on the upstream side. During upstream backfilling, slope failure occurred above the new culvert in May 2003 at the interface between unfrozen and partially frozen fill. A rehabilitation project was completed by removing part of the upstream fill and installing stone columns to reinforce the around the culvert.

4. Analysis and Discussion

Figure 8 gives the stability analysis of case studies for minimum FOS. For Vernon (British Columbia), slope stability analyses were conducted by varying the shear strength parameters and water table for both failure events. The minimum FOS based on extreme values ($c = 10$ kPa, $\phi = 33^\circ$, and water table at ground surface) was found to be 1.45 without berms and 2.24 with berms. This means that variation in soil properties and water table fluctuations were not the likely causes in both cases. Given the increased pore water pressure (confirmed by the reported piezometer data), the trigger mechanism in both cases was foundation failure. A gradual built up of excess pore water pressure in the foundation soil during construction decreased the effective stress that, in turn, decreased the shear strength (Terza-

ghi et al., 1996). Therefore, slope stability analysis alone is not capable because it precludes the stress-strain behavior of foundation soils.

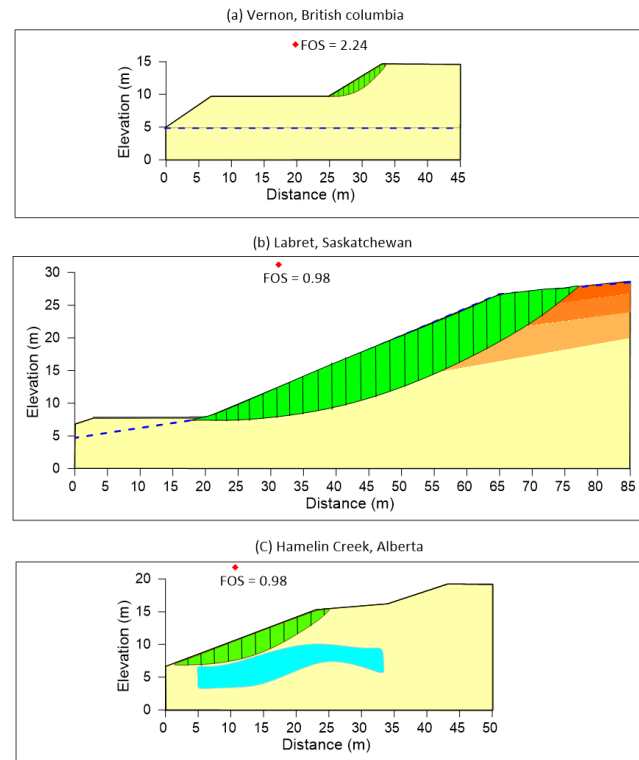


Figure 8. Stability analysis for minimum FOS: (a) Vernon, British Columbia; (b) Labret, Saskatchewan; (c) Hamelin Creek, Alberta.

For Labret (Saskatchewan), slope stability analyses were conducted with the reported soil properties of each layer along with variable water table (0 ~ 6 m from the slope surface) to capture the effect of rainfall. The FOS was found to be 0.98 for the water table at surface thereby corroborating the analysis of Donnelly et al. (2019). This confirms that the water table at surface saturated the entire slope thereby causing failure. The observed long-term rainfall facilitated gradual water infiltration into the soil to raise groundwater table up to the soil surface. This means that the driving force (soil weight) increased due to water weight and the resisting force (shear strength) decreased due to a reduced effective stress (Terzaghi et al., 1996). Transient soil-atmosphere interactions for identifying the phreatic surface could not be performed using the conventional slope stability method.

For Hamelin Creek (Alberta), slope stability analyses were conducted by varying soil properties and no water table. For the partially frozen soil, the shear parameters ($c = 40$ kPa and $\phi = 30^\circ$) were based on a similar soil (Huang et al., 2022). The FOS was found to be 0.98 for $c = 6$ kPa and $\phi = 18^\circ$ thereby validating the analysis of Tweedie et al. (2004). Ice formation resulted in a 10% volume increase in the soil that is partially recoverable during thawing albeit enlarged void spaces (Konrad and Mor-

genstern, 1984). In the soil profile, downward water movement was inhibited by the underlying frozen layer (Konrad and Samson, 2000; Zeinali et al., 2020). Gradual build up of pore water pressure at the frozen-unfrozen interface created a slip surface where the slope failed. Clearly, soil saturation along with pore pressure increase in the slope due to thawing of the frozen layer was the likely trigger mechanism.

5. Summary and Conclusions

Slope stability analysis are routinely conducted for the design of earthen embankments (such as hydraulic dams, tailing dams, highways, railways, and landfills) as well as for evaluating the integrity of natural hills. The geometrical configuration of all earth structure depends on spatially variable soil properties, site geology, regional climate, surface hydrology, and ground water table. Conventionally, the most stable slope is identified by analyzing critical cross-sections along the length of the structure. These cross-sections are selected using site conditions and engineering judgement. The main achievement of this research was to devise a systematic approach to capture the effects of field uncertainties for natural and manmade slopes. This approach for slope stability assessment is globally applicable provided the variations in site-specific conditions are effectively captured. The newly developed charts were made by changing slope geometry and randomly generating shear strength parameters. The subset simulation technique was used to determine the safe range of soil properties for various slopes. The design charts were validated using history matching of three failed slopes. These case studies were selected to understand the distinct trigger mechanisms resulting from construction practice, site geology, and environmental loading.

All of the slopes were found to be stable under the reported geometry and shear strength parameters while assuming no water table. Detailed investigations were conducted to capture the variation in soil properties and the effect of environmental conditions on water table. Results of the history matching are summarized as follows:

- At Vernon (British Columbia), increased pore water pressure during construction triggered foundation failure twice in the compacted fill over a glacial moraine tills.
- At Labret (Saskatchewan), saturation of the entire slope resulting from long duration rainfall triggered the slope failure in the natural cut with layered glacio-lacustrine clays.
- At Hamelin Creek (Alberta), soil saturation in the slope due to thawing of the frozen layer triggered the failure in the compacted fill on a glacial moraine till.

This validation illustrates that the new approach fully captures environmental loading (resulting in water table variation in the slope) and partly captures construction practice and site geology via soil properties. This approach can be extended to include other field conditions responsible for reducing FOS and arising from one or more of the following factors: (i) *Climate regimes* — Alternate freeze-thaw with 10% volume variation in cold climates lead to increased water flow due to enlarged pores. Similarly, cyclic saturation-desaturation in arid climates

develops soil cracks that serve as preferential flow paths. In humid climates, excessive rainfall ensures that the soil remains mostly saturated thereby decreasing the effective stress; (ii) *Extreme weather* — Long term droughts lead to soil cracking with the same effect as described before whereas flash floods facilitate water ponding on both sides of an embankment and results in lateral seepage forces causing internal erosion; (iii) *Geomorphology* — Effective stress is decreased by high runoff in mountain ranges as slopes are eroded to reduce the material weight and by high infiltration in rolling terrains where ponding results in water table rise; (iv) *Geology* — At a given effective stress, the shear strength of a sand (derived from ϕ) or a clay (derived from c) is always lower than natural soils; (v) *Loading* — Seismic activity results in a sudden loading on the soil such that pore water pressure cannot dissipate quickly thereby liquefying the soil. Likewise, repetitive and/or variable vehicular loading increases the driving force with respect to the material weight; (vi) *Contamination* — Deicing salts decrease c due to clay dispersion by the dissolved ions whereas landfill leachates reduce both c and ϕ due to bacterial and fungal growth.

Author contributions. R. Paranthaman: Data curation, Formal analysis, Investigation, Writing — original draft. S. Azam: Conceptualization, Funding acquisition, Supervision, Writing — review and editing. All authors have read and agreed to the published version of the manuscript.

Data availability statement. The data presented in this study are available in the figures and tables.

Conflicts of interest. The authors declare no conflict of interest.

Acknowledgements. This research was funded by Natural Sciences and Engineering Research Council of Canada, grant number RGPIN-06456-2018. The authors would like to acknowledge the University of Regina for providing laboratory space and computing facilities.

References

- Au, S.K. and Beck, J.L. (2003). Subset simulation and its application to seismic risk based on dynamic analysis. *Journal of Engineering Mechanics*, 129(8), 901-917. [https://doi.org/10.1061/\(ASCE\)0733-9399\(2003\)129:8\(901\)](https://doi.org/10.1061/(ASCE)0733-9399(2003)129:8(901))
- Bell, F.G. (2002). The geotechnical properties of some till deposits occurring along the coastal areas of eastern England. *Engineering Geology*, 63(1-2), 49-68. [https://doi.org/10.1016/S0013-7952\(01\)0068-0](https://doi.org/10.1016/S0013-7952(01)0068-0)
- Bogusz, W. and Godlewski, T. (2019). Philosophy of geotechnical design in civil engineering-possibilities and risks. *Bulletin of the Polish Academy of Sciences: Technical Sciences*, 67(2), 289-306. <https://doi.org/10.24425/bpas.2019.128258>
- Canada Weather Stats. Website name. <https://www.weatherstats.ca/?zoom=8;lat=50.45;long=-104.61> (accessed January 21, 2023)
- Cao, Z. (2012). *Probabilistic Approaches for Geotechnical Site Characterization and Slope Stability Analysis*. Ph.D. Dissertation, Department of Civil and Architectural Engineering, City University of Hong Kong, Hong Kong, China.
- Cao, Z. and Wang, Y. (2014). Bayesian model comparison and selection of spatial correlation functions for soil parameters. *Structural Safety*, 49, 10-17. <https://doi.org/10.1016/j.strusafe.2013.06.003>
- Carranza-Torres, C. and Hormazabal, E. (2018). Computational tools for the determination of factor of safety and location of the critical

- circular failure surface for slopes in Mohr-Coulomb dry ground. *Proceedings of the 2018 International Symposium of Slope Stability in Open Pit Mining and Civil Engineering*, Turin, September 21-24.
- Cheng, Y.M. and Lau, C.K. (2008). *Slope stability analysis and stabilization: New methods and insight*. CRC press, pp 78-36. ISBN: 0-203-92795-8
- Chowdhury, R. H. (2013). *Shear Strength of Compacted Expansive Soils*. M.Sc. Dissertation, Department of Environmental System Engineering, University of Regina, Regina, SK, Canada.
- Christian, J.T., Ladd, C.C. and Baecher, G.B. (1994). Reliability applied to slope stability analysis. *Journal of Geotechnical Engineering*, 120(12), 2180-2207. [https://doi.org/10.1061/\(ASCE\)0733-9410\(1994\)120:12\(2180\)](https://doi.org/10.1061/(ASCE)0733-9410(1994)120:12(2180))
- Clarke, B.G. (2018). The engineering properties of glacial tills. *Geotechnical Research*, 5(4), 262-277. <https://doi.org/10.1680/jgere.18.00020>
- Crawford, C.B., Fannin, R.J. and Kern, C.B. (1995). Embankment failures at Vernon, British Columbia. *Canadian Geotechnical Journal*, 32(2), 271-284. <https://doi.org/10.1139/t95-029>
- CSSS. Canadian Society of Soil Science. <https://csss.ca/> (accessed January 25, 2023)
- Das, B.M. and Sobhan, K. (2013). *Principles of geotechnical engineering*. Nelson Education, pp 469-523. ISBN: 978-1-305-97093-6
- Davies, T. (2015). Landslide hazards, risks, and disasters. In *Landslide Hazards, Risks, and Disasters*. Elsevier. pp 1-16. <https://doi.org/10.1016/B978-0-12-396452-6.00001-X>
- Donnelly, J., Singh, J. and Dhaliwal, R. (2019). *Lebret Landslide Mitigation Design Alternative*. Submitted to Faculty of Engineering and Applied Science, University of Regina, Regina, SK, Canada.
- El-Ramly, H., Morgenstern, N.R. and Cruden, D.M. (2002). Probabilistic slope stability analysis for practice. *Canadian Geotechnical Journal*, 39(3), 665-683. <https://doi.org/10.1139/t02-034>
- Glade, T. (2003). Vulnerability assessment in landslide risk analysis. *Erde*, 134(2), 123-146.
- Griffiths, D.V., Huang, J. and Fenton, G. A. (2009). Influence of spatial variability on slope reliability using 2-D random fields. *Journal of Geotechnical and Geoenvironmental Engineering*, 135(10), 1367-1378. [https://doi.org/10.1061/\(ASCE\)GT.1943-5606.0000099](https://doi.org/10.1061/(ASCE)GT.1943-5606.0000099)
- Harr, M.E. (1984). *Reliability-based design in civil engineering (Vol. 20)*. Department of Civil Engineering, School of Engineering, North Carolina State University, USA. pp 129-144. ISBN: 978-0-070-26697-1
- Hassan, A.M. and Wolff, T.F. (1999). Search algorithm for minimum reliability index of earth slopes. *Journal of Geotechnical and Geoenvironmental Engineering*, 125(4), 301-308. [https://doi.org/10.1061/\(ASCE\)10900241\(1999\)125:4\(301\)](https://doi.org/10.1061/(ASCE)10900241(1999)125:4(301))
- Hillel, D. (1998). *Environmental soil physics: Fundamentals, applications, and environmental considerations*. Elsevier Science. pp 341-378. ISBN: 978-0-12-348525-0
- Hoek, E. and Bray, J.D. (1981). *Rock Slope Engineering*. CRC Press. pp 341-351. ISBN: 0-419-16010-8
- Holtz, R.D., Kovacs, W.D. and Sheahan, T.C. (2011). *An introduction to geotechnical engineering (2nd edition)*. Prentice-Hall Englewood Cliffs. pp 733. ISBN: 0-13-484394-0
- Huang, W.J., Mao, X.S., Wu, Q. and Chen, L.L. (2022). Experimental study on shear characteristics of the silty clay soil-ice interface. *Scientific Reports*, 12(1), 19687. <https://doi.org/10.1038/s41598-022-23086-z>
- Huang, X.C. and Zhou, X.P. (2017). Reliability analysis of a large-scale landslide using SOED-based RSM. *Environmental Earth Sciences*, 76(23), 1-12. <https://doi.org/10.1007/s12665-017-7136-1>
- Jahnavi, T. (2016). *Reliability-Based Stability Analysis of Slope*. Master Dissertation, Department of Civil Engineering, National Institute of Technology, Rourkela, India.
- Jiang, S.H., Li, D.Q., Zhang, L.M., and Zhou, C.B. (2014). Slope reliability analysis considering spatially variable shear strength parameters using a non-intrusive stochastic finite element method. *Engineering Geology*, 168(16), 120-128. <https://doi.org/10.1016/j.enggeo.2013.11.006>
- Johari, A. and Javadi, A.A. (2012). Reliability assessment of infinite slope stability using the jointly distributed random variables method. *Scientia Iranica*, 19(3), 423-429. <https://doi.org/10.1016/j.scient.2012.04.006>
- Johari, A. and Khodaparast, A.R. (2013). Modelling of probability liquefaction based on standard penetration tests using the jointly distributed random variables method. *Engineering Geology*, 158, 1-14. <https://doi.org/10.1016/j.enggeo.2013.02.007>
- Johari, A. and Mousavi, S. (2019). An analytical probabilistic analysis of slopes based on limit equilibrium methods. *Bulletin of Engineering Geology and the Environment*, 78(6), 4333-4347. <https://doi.org/10.1007/s10064-018-1408-1>
- Konrad, J.M. and Morgenstern, N.R. (1984). Frost heave prediction of chilled pipelines buried in unfrozen soils. *Canadian Geotechnical Journal*, 21(1), 100-115. <https://doi.org/10.1139/t84-008>
- Konrad, J.M. and Samson, M. (2000). Influence of freezing temperature on hydraulic conductivity of silty clay. *Journal of Geotechnical and Geoenvironmental Engineering*, 126(2), 180-187. [https://doi.org/10.1061/\(ASCE\)1090-0241\(2000\)126:2\(180\)](https://doi.org/10.1061/(ASCE)1090-0241(2000)126:2(180))
- Li, D.Q., Chen, Y.F., Lu, W.B. and Zhou, C.B. (2011). Stochastic response surface method for reliability analysis of rock slopes involving correlated non-normal variables. *Computers and Geotechnics*, 38(1), 58-68. <https://doi.org/10.1016/j.compgeo.2010.10.006>
- Li, D.Q., Xiao, T., Cao, Z.J., Zhou, C.B. and Zhang, L.M. (2016). Enhancement of random finite element method in reliability analysis and risk assessment of soil slopes using Subset Simulation. *Landslides*, 13(2), 293-303. <https://doi.org/10.1007/s10346-015-0569-2>
- Li, K.S. (1992). Point-estimate method for calculating statistical moments. *Journal of Engineering Mechanics*, 118(7), 1506-1511. [https://doi.org/10.1061/\(ASCE\)0733-9399\(1992\)118:7\(1506\)](https://doi.org/10.1061/(ASCE)0733-9399(1992)118:7(1506))
- Low, B.K., Gilbert, R.B. and Wright, S.G. (1998). Slope reliability analysis using generalized method of slices. *Journal of Geotechnical and Geoenvironmental Engineering*, 124(4), 350-362. [https://doi.org/10.1061/\(ASCE\)1090-0241\(1998\)124:4\(350\)](https://doi.org/10.1061/(ASCE)1090-0241(1998)124:4(350))
- Low, B.K. and Tang, W.H. (2007). Efficient spreadsheet algorithm for first-order reliability method. *Journal of Engineering Mechanics*, 133(12), 1378-1387. [https://doi.org/10.1061/\(ASCE\)0733-9399\(2007\)133:12\(1378\)](https://doi.org/10.1061/(ASCE)0733-9399(2007)133:12(1378))
- Malkawi, A.I.H., Hassan, W.F. and Abdulla, F.A. (2000). Uncertainty and reliability analysis applied to slope stability. *Structural Safety*, 22(2), 161-187. [https://doi.org/10.1016/S0167-4730\(00\)00006-0](https://doi.org/10.1016/S0167-4730(00)00006-0)
- MDH. (2010). *Saskatchewan Metals Processing Plant — Geotechnical Investigation for Storage Facilities*. MDH engineering solutions. pp 10-25.
- Mitchell, J. K. and Soga, K. (2005). *Fundamentals of Soil Behavior*. John Wiley & Sons New York. pp 255-269. ISBN: 978-0-471-46302-3
- Morgenstern, N.R. and Price, V.E. (1965). The Analysis of the Stability of General Slip Surfaces. *Geotechnique*, 15(1), 79-93. <https://doi.org/10.1680/geot.1965.15.1.79>
- Oh, W.T. and Vanapalli, S.K. (2010). Influence of rain infiltration on the stability of compacted soil slopes. *Computers and Geotechnics*, 37(5), 649-657. <https://doi.org/10.1016/j.compgeo.2010.04.003>
- Tang, W.H., Yucemen, M.S. and Ang, A.S. (1976). Probability-based short term design of soil slopes. *Canadian Geotechnical Journal*, 13(3), 201-215. <https://doi.org/10.1139/t76-024>
- Terzaghi, K., Peck, R.B. and Mesri, G. (1996). *Soil Mechanics in Engineering Practice*. John Wiley and Sons. pp 83-116. ISBN: 0-471-08658-4
- Transportation Safety Board. (2013). *Subgrade collapse and derailment, Togo, Saskatchewan (Railway investigation report R13W0124)*, Transportation Safety Board of Canada.
- Tweedie, R., Clementino, R., Papanicolas, D., Skirrow, R. and Moser, G. (2004). Stabilization of a highway embankment fill over an arch

- culvert using stone columns. *57th Canadian Geotechnical Conference*, Quebec City, 24-31.
- Vanapalli, S.K., Fredlund, D.G. and Pufahl, D.E. (1997). Comparison of saturated-unsaturated shear strength and hydraulic conductivity behavior of a compacted sandy-clay till. *In Proceedings of the 50th Canadian Geotechnical Conference*, Ottawa, 20-22.
- Wang, J. P. and Huang, D.R. (2012). RosenPoint: A Microsoft Excel-based program for the Rosenblueth point estimate method and an application in slope stability analysis. *Computers and Geosciences*, 48, 239-243. <https://doi.org/10.1016/j.cageo.2012.01.009>
- Wang, X.B., Ramly, H.E., Proudfoot, D. and Skirrow, R. (2012). *Alberta Highway 858: 02 Embankment Stabilization — Geotechnical Investigation, Design, and Construction*. Proceedings of Landslides and Engineered Landslides: Protecting Society through Improved Understanding, pp 1509-1514. ISBN: 978-0-415-62123-6
- Wang, Y., Cao, Z. J. and Au, S.K. (2011). Practical reliability analysis of slope stability by advanced Monte Carlo simulations in a spreadsheet. *Canadian Geotechnical Journal*, 48(1), 162-172. <https://doi.org/10.1139/T10-044>
- Wyllie, D.C. (2018). *Rock Slope Engineering Civil Applications Fifth Edition*: Boca Raton, CRC Press, pp 239-264. ISBN: 978-1-4987-8627-0
- Zeinali, A., Edeskär, T. and Laue, J. (2020). Mechanism of thawing. *Cogent Engineering*, 7(1), 1716438. <https://doi.org/10.1080/23311916.2020.1716438>
- Zhang, J., Zhang, L.M. and Tang, W.H. (2011). New methods for system reliability analysis of soil slopes. *Canadian Geotechnical Journal*, 48(7), 1138-1148. <https://doi.org/10.1139/t11-009>
- Zhou, X.P. and Huang, X.C. (2018). Reliability analysis of slopes using UD-based response surface methods combined with LASSO. *Engineering Geology*, 233, 111-123. <https://doi.org/10.1016/j.enggeo.2017.12.008>